

# SIMO detection schemes for underwater optical wireless communication under turbulence

Weihao Liu,<sup>1,2</sup> Zhengyuan Xu,<sup>1,3,\*</sup> and Liuqing Yang<sup>4</sup>

<sup>1</sup>School of Information Science and Technology, University of Science and Technology of China, Hefei, China

<sup>2</sup>State Key Laboratory of Robotics, Shenyang Institute of Automation, Chinese Academy of Sciences, Shenyang, China

<sup>3</sup>Key Laboratory of Wireless-Optical Communications, Chinese Academy of Sciences, Hefei, China

<sup>4</sup>Department of Electrical and Computer Engineering, Colorado State University, Fort Collins, Colorado 80521, USA

\*Corresponding author: xuzhy@ustc.edu.cn

Received October 21, 2014; revised December 2, 2014; accepted December 14, 2014;  
posted January 27, 2015 (Doc. ID 225438); published April 6, 2015

In underwater optical wireless communication (UOWC), a channel is characterized by abundant scattering/absorption effects and optical turbulence. Most previous studies on UOWC have been limited to scattering/absorption effects. However, experiments in the literature indicate that underwater optical turbulence (UOT) can cause severe degradation of UOWC performance. In this paper, we characterize an UOWC channel with both scattering/absorption and UOT taken into consideration, and a spatial diversity receiver scheme, say a single-input-multiple-output (SIMO) scheme, based on a light-emitting-diode (LED) source and multiple detectors is proposed to mitigate deep fading. The Monte Carlo based statistical simulation method is introduced to evaluate the bit-error-rate performance of the system. It is shown that spatial diversity can effectively reduce channel fading and remarkably extend communication range. © 2015 Chinese Laser Press

OCIS codes: (010.4455) Oceanic propagation; (060.0060) Fiber optics and optical communications.

<http://dx.doi.org/10.1364/PRJ.3.000048>

## 1. INTRODUCTION

Underwater exploration has always been a very attractive topic to researchers worldwide, because tremendous unexplored undersea resources will be good complements for the shortage of land resources [1]. High-speed underwater wireless communication (UWC) is essential for efficient underwater exploration. However, due to strong water attenuation, radio-frequency-based communication technologies that are widely applied in terrestrial environments, are rarely used for UWC [2]. Acoustic waves are traditionally used for establishing relatively long-range wireless underwater links. Recently developed single-carrier and multicarrier modulation techniques [3–5] have significantly improved traditional modulation counterparts, in terms of communication range and data rate. Their data rates are of the order of tens of kilobits per second. But there is still demand for high-rate communication at short distances, such as in sensor networks of for diver communication. Meanwhile, the large apparatus of an acoustic-based UWC system is highly energy consuming and inconvenient for operation. It is imperative to explore new and alternative means for real-time high-rate UWC, especially along with the advancement of underwater unmanned vehicles.

Underwater optical wireless communication (UOWC), which uses the light transmission window of water in the 400–600 nm (blue/green) wavelength band, turns out to be an appropriate solution for real-time high-rate communication up to 1 Gbps in meters and 10 Mbps in hundreds of meters [6–9], and allows underwater transmission of data, images, and even video.

However, UOWC is also subject to great challenges since the optical beam is attenuated significantly by the scattering and absorption effects of water's molecular and suspending

particles, such as chlorophyll, water soluble salts, and minerals. Multiple scattering will increase the path loss and expand the impulse response, which causes intersymbol interference when transmitting high data rates or over long distances [6,10]. It is thus important to accurately characterize the UOWC channel and optimize channel utilization. Extensive research has been carried out on this topic. The authors of Refs. [11,12] studied the impulse response for the line-of-sight (LOS) UOWC channel, and Ref. [13] reports study of the change of polarization state as the light propagates in the scattering channel.

In addition to scattering/absorption effects, the UOWC suffers from serious underwater optical turbulence (UOT), which is physically the refractive index fluctuation of water with random variations of temperature and pressure. The UOT will cause fluctuation (scintillation) of received signals and result in link outage. Yet, unfortunately, to date the UOT is still an undeveloped field in UOWC. Preliminary studies about UOT were carried out in Ref. [14] for the underwater optical image system, and it showed that turbulence greatly degrades image quality by causing wandering and scintillation of the image. These effects are actually unavoidable in UOWC and will greatly degrade communication quality, as well.

In this paper, we will specifically study UOWC channel characteristics with both scattering/absorption and turbulence taken into consideration. In order to reduce the signal scintillation caused by UOT and to mitigate channel fading, we propose to use a spatial diversity receiver, namely, a single-input-multiple-output (SIMO) system. The system bit-error-rate (BER) performance will be evaluated.

The paper is organized as follows. Section 2 presents the signal propagation model of UOWC in the UOT and

scattering/absorption channel. Section 3 introduces the proposed SIMO scheme. In Sections 4 and 5 we perform numerical and analytical studies of BER performance under different conditions such as turbulence, communication range, and receiver diversity. Section 6 concludes this paper.

## 2. UNDERWATER OPTICAL WIRELESS PROPAGATION MODEL

When propagating through the underwater channel with scattering/absorption and UOT, both attenuation and fading will be added into the transmitted signals. Under this condition, the signal light intensity that can be received should be expressed as

$$I_r = I_t \cdot P_l \cdot I, \quad (1)$$

where  $I_t$  is the transmitted signal intensity,  $P_l$  represents the mean attenuation (path loss) caused by scattering/absorption effects and beam expansion, which reduces the mean irradiance of the light beam, and  $I$  signifies the normalized channel fading, which satisfies a certain probability distribution function (PDF)  $f(I)$  under the influence of UOT. In the following two sub-sections, we will discuss the factors of  $f(I)$  and  $P_l$ , respectively.

### A. UOT Model

As is well known, atmospheric optical turbulence (AOT) has been extensively studied for several decades in free-space optical (FSO) communications, and both theories and experimental studies have been well developed. Since the physical mechanism of UOT is similar to that of AOT, i.e., they are both caused mainly by the random variations of temperature and pressure of the medium [15], the classical theory of AOT can naturally be used for studies of UOT. According to the theory of AOT, the spectrum density of the medium, which is the Fourier representation of the variation of refractive index, is the primary indicator of the property of the optical turbulence. Following the classical Kolmogorov spectrum model of AOT, the spectrum density of UOT can be expressed as [14]

$$\Phi_n^K(\kappa) = K_3 \kappa^{-11/3}, \quad (2)$$

where  $K_3 = \chi \varepsilon^{-1/3}$  ( $\chi$  expresses the strength of temperature gradient and  $\varepsilon$  is the kinetic energy dissipation rate) is the constant that determines the turbulence strength, and it is similar to  $C_n^2$  in AOT [16]. For underwater conditions, its value ranges from  $10^{-14}$  to  $10^{-8} \text{ m}^{-2/3}$ , several orders larger than the  $C_n^2$  value in AOT. This is because  $K_3$  and  $C_n^2$  are physically in correlation with the refractive index variation ( $\Delta n$ ) of the medium, and for underwater conditions,  $\Delta n$  is typically several orders larger than that in the atmosphere [17]. It should be noted that Eq. (2) represents only the spectrum density of the medium in the inertial turbulence region, and it ignores the effects of the inner scale and outer scale of turbulence [18].

Optical turbulence will result in the random fluctuation of received light intensity, which is quantitatively represented by the PDF and scintillation index. For AOT, three PDF models are commonly adopted, namely, lognormal distribution, K-distribution, and Gamma-Gamma (GG) distribution [19], where the former two models are suitable for weak turbulence and the latter applies from weak to strong turbulence.

In practical applications of UOWC, the front end of a detector is usually an optical lens with a specific aperture dimension that is much larger than the light's transversal coherent length. Under this condition, the fluctuation of received light will be remarkably weakened by the aperture averaging effect [19]. Large numbers of field experiments have shown that, considering the aperture averaging effect, the PDF of received light intensity in AOT can be well represented by the lognormal distribution function even for strong turbulence conditions [20]. Analogously, the PDF  $f(I)$  for the UOT channel can also be expressed as the lognormal function

$$f(I) = \frac{1}{I \sigma \sqrt{2\pi}} \exp\left(-\frac{(\ln(I/I_0) - \mu)^2}{2\sigma^2}\right), \quad (3)$$

where  $I_0$  is the mean received light intensity,  $\mu$  is the mean logarithmic light intensity, and  $\sigma^2$  is the scintillation index defined by

$$\sigma^2 = \frac{\langle I^2 \rangle - \langle I \rangle^2}{\langle I \rangle^2}. \quad (4)$$

Here,  $\langle \cdot \rangle$  is the mean operator. Normalization of Eq. (3) leads to  $\mu = -\sigma^2/2$ . For a plane wave,  $\sigma^2$  can be expressed as [19]

$$\sigma^2 = \exp\left[\frac{0.49\sigma_r^2}{(1 + 1.11\sigma_r^{12/5})^{7/6}} + \frac{0.51\sigma_r^2}{(1 + 0.69\sigma_r^{12/5})^{5/6}}\right] - 1, \quad (5)$$

where  $\sigma_r^2$  is the Rytov variance. Based on the traditional FSO theory of AOT, in combination with the UOT spectrum model defined by Eq. (2), it can be expressed as [19]

$$\sigma_r^2 = 37.3K_3 \left(\frac{2\pi}{\lambda}\right)^{7/6} L^{11/6}, \quad (6)$$

where  $\lambda$  is the wavelength and  $L$  is the migration length of the light beam.

### B. Underwater Scattering/Absorption Channel Model

Light scattering/absorption from underwater suspended particulates and the expansion of emitted light beams are the two primary factors that result in path loss of the UOWC channel, and they are also the major topics of previous studies for characterizing the UOWC channel. The Monte Carlo (MC) ray-tracing method is an effective way to obtain the channel properties, such as path loss and impulse response [21,22]. For the scattering/absorption channel, the channel characteristics are largely determined by the optical properties of water and by the system parameters of the UOWC links, such as the beam divergent angle, communication range, and field of view (FOV) of the receiver. In this paper, we will use the MC ray-tracing method and largely follow the simulation procedures of Refs. [21,22] to evaluate the path loss performance, namely,  $P_l$  in Eq. (1), of the UOWC channel.

## 3. SCHEME OF SIMO-UOWC

As in traditional FSO communication and wireless communication, UOT and multiple scattering will cause deep fading of received signals and communication outage. To mitigate deep fading, in this section we introduce a spatial diversity receiver and propose a SIMO transceiver scheme for UOWC.

In traditional wireless communication, spatial diversity has been widely used to avoid deep fading. To achieve the best performance, the subchannels of the SIMO system should be independent of each other, i.e., the receiver separation should be larger than the transversal coherent length  $\rho_0$ , defined as the distance between two transversal positions where the correlation coefficient is less than  $1/e$ . So,  $\rho_0$  is a key parameter of the system. Again using the traditional FSO theory of AOT together with the UOT spectrum model,  $\rho_0$  in the SIMO-UOWC system can be obtained [19]:

$$\rho_0 = \left( 44.2K_3 \left( \frac{2\pi}{\lambda} \right)^2 L \right)^{-3/5}. \quad (7)$$

Based on Eq. (7), the coherent length of a light beam versus the propagation length in UOT of different turbulence strengths can be obtained, as shown in Fig. 1, where  $\lambda$  is 530 nm. We can see that  $\rho_0$  decreases gradually with propagation length and turbulence strength, and it is much less than 1 cm when the propagation length is larger than 30 m in moderate to strong turbulence. That means the independent fading subchannels can be obtained once the transversal distance between detectors is larger than 1 cm. This is not difficult to realize in field experiments and applications.

The proposed schematic diagram of the SIMO-UOWC transceiver system is shown in Fig. 2, where the detectors are distributed as a concentric circle on the receiving plane. For practical application and cost considerations, the ordinary light-emitting-diode (LED) with a certain beam divergence is used as the light source. To enhance the aperture averaging effect and meet the diversity requirement, the dimension of each receiving optical lens is set as  $D = 3\text{--}5$  cm, and the central distance between adjacent lenses is  $d = 5\text{--}10$  cm. It should be noted that an optical lens with an extremely large aperture is very difficult to manufacture in reality, which is why we use the combination of aperture averaging and spatial diversity here. Previous studies [23] showed that the differences of mean light intensities received by different detectors are insignificant provided every detector is in the light cone of the transmitter, i.e., the transmitter and all detectors form LOS subchannels.

For the combining scheme at the receiver, we will consider maximum ratio combining (MRC) which is based on the

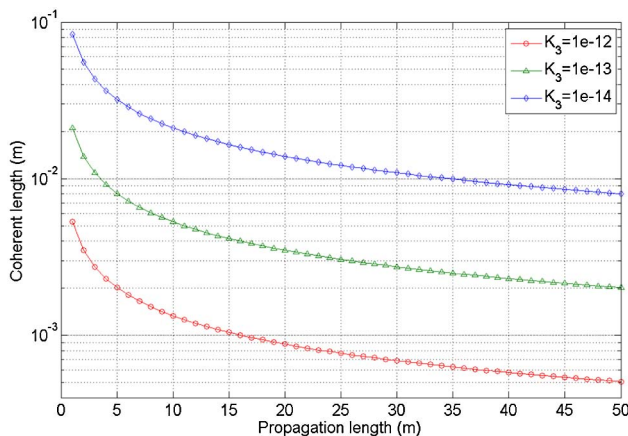


Fig. 1. Coherent length versus propagation length as a function of UOT strength.

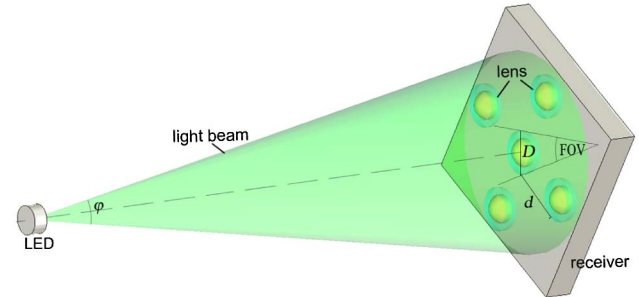


Fig. 2. Proposed SIMO transceiver system for UOWC.

maximum likelihood decision rule [24], selection combining (SC), and equal gain combining (EGC). They will be studied in detail in the next section.

#### 4. BER PERFORMANCE UNDER TURBULENCE

In this section, we use the MC statistical simulation method to evaluate the BER performance of the proposed SIMO-UOWC system with different combining schemes. We consider the intensity-modulation/direct-detection (IM/DD) links using on-off keying (OOK). The receivers are the photon detectors that transform the light into electrical currents. The output of each detector can be expressed as

$$r = \eta(I_r + I_b) + n, \quad (8)$$

where  $\eta$  is the optical-to-electrical conversion coefficient,  $I_r$  is the received signal light intensity expressed by Eq. (1),  $I_b$  is ambient light intensity, and  $n$  is the additive white Gaussian noise with zero mean and variance of  $N_0/2$  ( $N_0$  is the thermal noise power spectrum defined by  $N_0 = 4KT B/R$ , where  $K$  is the Boltzmann constant, and  $R$ ,  $T$ , and  $B$  are, respectively, the receiver resistance, temperature in Calvin, and the electrical receiver bandwidth). It has been proven that, for underwater scenarios, the dominant noise is electrical thermal noise [25]. The interference from  $I_b$  is insignificant and can be effectively filtered out by the optical filters. Therefore, in this paper we will consider only thermal noise.

As is well known, for a SISO system, the mean BER for the IM/DD-OOK system in a fading channel can be expressed as

$$p_e = \int_0^\infty f(I_r) Q\left(\frac{\eta I_r}{\sqrt{2N_0}}\right) dI_r, \quad (9)$$

where  $Q(\cdot)$  is the Gaussian  $Q$  function, and  $f(I_r)$  is the PDF expressed by Eq. (3) with the mean received intensity  $I_0$  depending on the transmitted signal intensity  $I_t$  and channel attenuation  $P_t$ . In obtaining Eq. (9), the transmission probabilities of *on* and *off* are assumed to be the same, and the decision threshold is  $I_0/2$ .

Following Eq. (9), the BER expressions of the SIMO-UOWC system under different receiver combining schemes can be obtained. For the SIMO system with MRC receivers, the mean BER can be expressed as [24]

$$p_e = \int_0^\infty f(I_r) Q\left(\frac{\eta}{\sqrt{2MN_0}} \sqrt{\sum_{i=1}^M I_i^2}\right) dI_r, \quad (10)$$

where  $I_i$  is the light received by the  $i$ th detector and  $M$  is the number of detectors. For EGC, it changes to

$$p_e = \int_0^\infty f(I_r) Q\left(\frac{\eta}{M\sqrt{2N_0}} \sum_{i=1}^M I_i\right) dI_r. \quad (11)$$

For the SC receiver, the mean BER is

$$p_e = \int_0^\infty f(I_r) Q\left(\frac{\eta I_r}{\sqrt{2MN_0}}\right) dI_r, \quad (12)$$

where

$$I_r = \max(I_1, I_2, \dots, I_M). \quad (13)$$

For the three combining schemes listed above, the MRC needs to have full knowledge of the SNR level of every receiving branch, which usually requires a complicated transceiver system. The EGC is easy to realize and is most commonly used in real applications. The SC receiver is the least complicated since it processes only one of the diversity apertures (the aperture with the maximum received intensity).

In the following, we will consider the dependence of the mean BERs expressed by Eqs. (10)–(12) on the mean SNR at the receiver. The real propagation properties of light in the UOT and attenuation channel will be ignored and will be studied in the next section. In reality, calculation of Eqs. (10)–(12) is usually quite tedious since there are no closed forms for the lognormal channel. Previously, much effort was spent on their analytical simplification, and usually some approximations should be used [24]. In this paper, we will introduce the MC statistical simulation method to get the mean BER of the fading channel as below. For each individual receiving branch, namely the  $j$ th branch, we launch large numbers of samples,  $n_s$  samples, of the received signal intensity  $I_{rij}$  ( $i = 1, 2, \dots, n_s$ ) that satisfies the PDF of  $f(I_r)$ , in which the mean intensity  $I_0$ , essentially determined by  $I_t$  and  $P_l$ , is properly chosen to get the SNR of each sample as follows:

$$\text{SNR}_{ij} = \frac{2\eta^2 I_{rij}^2}{N_0}, \quad (14)$$

The mean SNR can be obtained by averaging over all samples:

$$\overline{\text{SNR}} = \frac{1}{Mn_s} \sum_{j=1}^M \sum_{i=1}^{n_s} \text{SNR}_{ij}. \quad (15)$$

To get the BER of the SIMO system, we combine samples from all receiving branches, respectively, by using the MRC, EGC, and SC schemes, respectively, to form a combined sample  $I_{rci}$ . The BER for each combined sample can be obtained from

$$\text{BER}_i = Q\left(\frac{\eta I_{rci}}{\sqrt{2N_0}}\right). \quad (16)$$

The mean BER of the system can then be obtained by averaging the total  $n_s$  combined samples:

**Table 1. Simulation Parameters**

	$\lambda$	$\phi$	FOV	$D$	$d$
System parameters	530 nm	20°	60°	5 cm	10 cm
Receiving electrical parameters		$\eta$	$R$	$T$	$B$
		0.35 A/W	1 M $\Omega$	300 K	150 MHz

$$\overline{\text{BER}} = \frac{1}{n_s} \sum_{i=1}^{n_s} \text{BER}_i, \quad (17)$$

For a SISO system, we set  $M = 1$  in Eq. (15) and  $I_{rci} = I_{rij}$  in Eq. (16).

The receiver electrical parameters used in all simulations in this paper are given in Table 1. The simulation results of the mean BER in terms of the mean SNR for different combining schemes with receiving branches  $M = 3, 5$  are given in Fig. 3, where  $K_3 = 10^{-12} \text{ m}^{-2/3}$ , indicating strong UOT. To achieve the same BER, the required mean SNR for the SIMO system can be remarkably reduced compared with that for the SISO system, and this reduction increases with branch number  $M$  (approximately 10 dB for  $M = 3$  and 15 dB for  $M = 5$ ). The BER–SNR curves of the MRC and EGC schemes almost overlap each other except under the high SNR condition, where MRC outperforms EGC. They both outperform SC.

Figure 4 shows the mean BER in terms of the mean SNR for different turbulence strengths and different combining

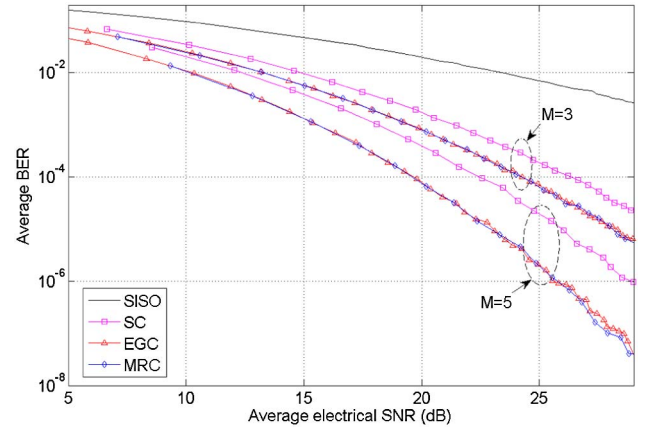


Fig. 3. Mean BER versus mean SNR for different combining schemes with  $M = 3$  and  $M = 5$ .

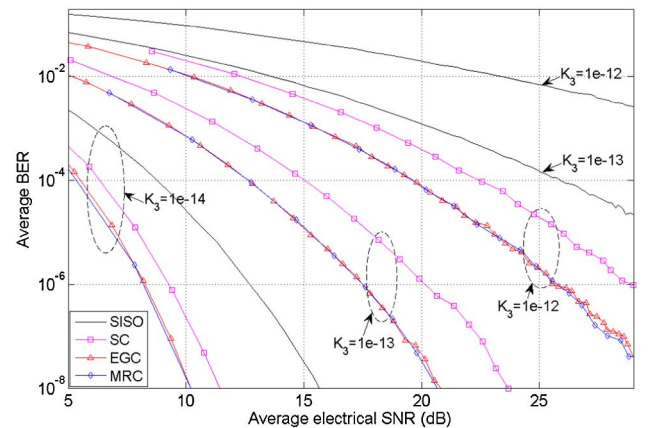


Fig. 4. Mean BER versus mean SNR for different UOT strengths.

schemes. Here  $M = 5$ . It indicates that, to get the same BER level, the required SNR increases remarkably with turbulence strength: the required SNR in a strong UOT channel ( $K_3 = 10^{-12} \text{ m}^{-2/3}$ ) is 20 dB larger than that in a weak UOT channel ( $K_3 = 10^{-14} \text{ m}^{-2/3}$ ), as shown in the figure.

## 5. BER PERFORMANCE UNDER ATTENUATION AND TURBULENCE

In this section, we combine the scattering/absorption effects and UOT of the UOWC channel to evaluate the communication performance of the proposed SIMO-UOWC system, i.e., we will consider both the path loss  $P_l$  and fading of the channel. As stated in Section 2, path loss  $P_l$  can be obtained by using the MC ray-tracing method. The simulation system parameters are given in Table 1, and clear ocean water with the optical properties given in Ref. [22] is considered. Under this condition, the scattering by suspended particles is not so significant and UOT is the dominant factor in the channel. We assume that the fading property of the channel is not influenced by scattering/absorption effects, so the PDF of Eq. (3) can still be used. This is similar to the case in which a laser propagates in clear air where the optical turbulence effect is dominant [16].

Figure 5 presents the simulation results of the mean BER with varying propagation distance of light in water with strong UOT ( $K_3 = 10^{-12} \text{ m}^{-2/3}$ ) as functions of receiving branches and of combining schemes. If we set the threshold BER to be  $10^{-6}$ , the effective communication range for the SISO system is less than 40 m, while for the SIMO system, this range can reach more than 60 m for the MRC scheme. More receiving branches mean longer communication range.

Figure 6 shows the BER performance in different UOT strengths. Here  $M = 5$  for the SIMO schemes and the transmitting signal power is  $I_t = 1 \text{ W}$ . For comparison, the result for the SISO case under the traditional UOWC channel without considering UOT is also shown. We can see that, for the SISO system, the effective communication range in the non-UOT condition is about 5 m longer than that in the weak UOT condition, and they both extend to more than 20 m longer than that in strong UOT. However, for the SIMO system, the differences between weak and strong turbulence channels

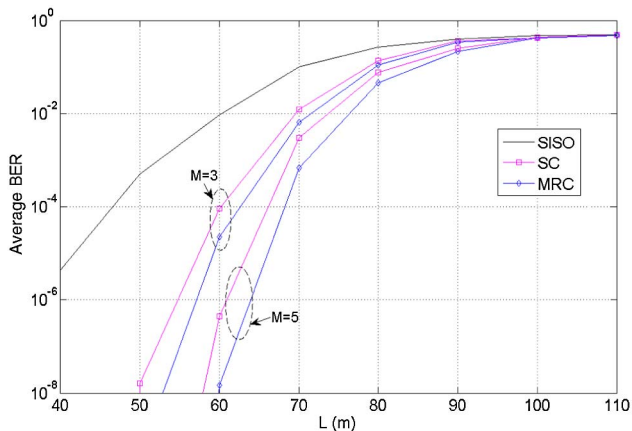


Fig. 5. Mean BER versus communication range for different combining schemes under attenuation and turbulence. The transmitting power is  $I_t = 1 \text{ W}$ .

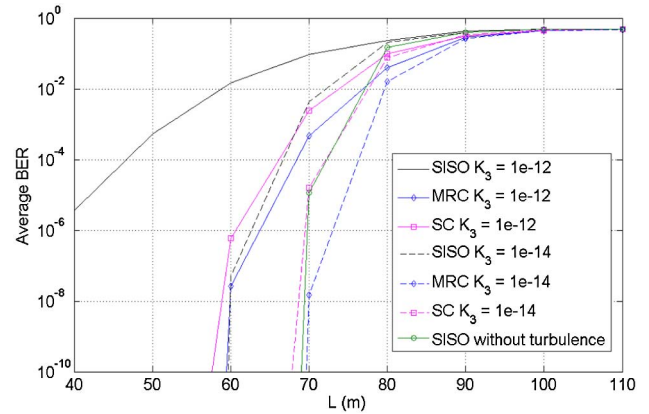


Fig. 6. Mean BER versus communication range for different combining schemes under different turbulence.

reduces to less than 10 m. These results indicate that the SIMO system is an effective way to mitigate strong UOT.

Note that, in this paper we consider only the case in which the scattering/absorption effects contributed by suspended particles are insignificant and UOT dominates the fading characteristics of the channel. While the scattering is significant, such as in coastal or harbor waters, which are filled with large amounts of suspended particulates, the scattering will become dominant. Under these conditions, the fluctuation of received light intensity due to channel fading will be greatly smoothed by scattering [26]. Following the studies of scattering and the AOT channel in the atmosphere, it is conjectured that the PDF of the received light intensity can be well approximated by the lognormal distribution, but with scintillation index  $\sigma^2$  much less than that given by Eq. (5). Further studies on this topic will be carried out in the future.

## 6. CONCLUSION

An UOWC channel with both scattering/absorption and UOT is characterized, and a SIMO scheme is proposed to mitigate the deep fading of the turbulence channel. A statistical MC simulation method is introduced to evaluate the BER performance of the system. The simulation results show that, compared with the SISO system, the required SNR reduction of more than 15 dB and communication range increase of more than 30 m can be obtained at a target BER of  $10^{-6}$  by using five receiving apertures. Using the SIMO system, an LED with 1 W optical power can reach an effective communication range of more than 60 m in a strong UOT channel, indicating promising applications in LED-based UOWC.

## ACKNOWLEDGMENTS

This work was supported by the National Key Basic Research Program of China (Grant No. 2013CB329201), the National Natural Science Foundation of China (Grant Nos. 61171066 and 61471332), and the State Key Laboratory of Robotics.

## REFERENCES

1. I. Vasilescu, C. Detweiler, and D. Rus, "AquaNodes: an underwater sensor network," in *Proceedings of the Second Workshop on Underwater Networks* (ACM, 2007), pp. 85–88.
2. B. M. Cochenour, L. J. Mullen, and A. E. Laux, "Characterization of the beam-spread function for underwater wireless optical

- communications links," *IEEE J. Ocean. Eng.* **33**, 513–521 (2008).
3. X. Cheng, F. Qu, and L. Yang, "Single carrier FDMA over underwater acoustic channels," in *Proceedings of Communications and Networking in China (CHINACOM)* (IEEE, 2011), pp. 1052–1057.
  4. B. Li, S. Zhou, M. Stojanovic, L. Freitag, and P. Willett, "Multi-carrier communication over underwater acoustic channels with nonuniform Doppler shifts," *IEEE J. Ocean. Eng.* **33**, 198–209 (2008).
  5. X. Cheng, M. Wen, X. Cheng, L. Yang, and Z. Xu, "Effective self-cancellation of intercarrier interference for OFDM underwater acoustic communications," in *Proceedings of the 8th ACM International Conference on Underwater Networks & Systems* (2013).
  6. F. Hanson and S. Radic, "High bandwidth underwater optical communication," *Appl. Opt.* **47**, 277–283 (2008).
  7. M. Doniec and D. Rus, "BiDirectional optical communication with AquaOptical II," in *Proceedings of IEEE International Conference on Communication Systems (ICCS)* (IEEE, 2009), pp. 390–394.
  8. M. Doniec, I. Vasilescu, M. Chitre, C. Detweiler, M. Hoffmann-Kuhnt, and D. Rus, "AquaOptical: a lightweight device for high-rate long-range underwater point-to-point communication," in *Proceedings of OCEANS 2009, MTS/IEEE Biloxi-Marine Technology for Our Future: Global and Local Challenges* (IEEE, 2009), pp. 1–6.
  9. D. Anguita, D. Brizzolaro, and G. Parodi, "Building an underwater wireless sensor network based on optical communication: Research challenges and current results," in *Proceedings of Third International Conference on Sensor Technologies and Applications* (IEEE, 2009), pp. 476–479.
  10. C. D. Mobley, *Light and Water: Radiative Transfer in Natural Waters* (Academic, 1994).
  11. C. Gabriel, M. A. Khalighi, S. Bourennane, P. Léon, and V. Rigaud, "Channel modeling for underwater optical communication," in *Proceedings of IEEE GLOBECOM Workshops on Optical Wireless Communications* (IEEE, 2011), pp. 833–837.
  12. F. Schill, U. R. Zimmer, and J. Trumpf, "Visible spectrum optical communication and distance sensing for underwater applications," in *Proceedings of Australian Conference on Robotics and Automation (ACRA)* (2004).
  13. S. Jaruwatanadilok, "Underwater wireless optical communication channel modeling and performance evaluation using vector radiative transfer theory," *IEEE J. Sel. Areas Commun.* **26**, 1620–1627 (2008).
  14. W. Hou, "A simple underwater imaging model," *Opt. Lett.* **34**, 2688–2690 (2009).
  15. J. A. Domaradzki, "Light scattering induced by turbulence flow: a numerical study," Tech. Rep. N00014-96-0420 (University of Southern California, 1997).
  16. L. C. Andrews and R. L. Phillips, *Laser Beam Propagation Through Random Media* (SPIE, 2005).
  17. D. J. Bogucki, J. A. Domaradzki, C. Anderson, H. W. Wijesekera, J. R. V. Zaneveld, and C. Moore, "Optical measurement of rates of dissipation of temperature variance due to oceanic turbulence," *Opt. Express* **15**, 7224–7230 (2007).
  18. A. Ishimaru, *Wave Propagation and Scattering in Random Media* (Academic, 1978).
  19. L. C. Andrews, R. L. Phillips, and C. Y. Hopen, *Laser Beam Scintillation with Applications* (SPIE, 2001).
  20. F. S. Vetelino, C. Young, L. Andrews, and J. Reolons, "Aperture averaging effects on the probability density of irradiance fluctuations in moderate-to-strong turbulence," *Appl. Opt.* **46**, 2099–2108 (2007).
  21. H. Ding, G. Chen, A. K. Majumdar, B. M. Sadler, and Z. Xu, "Modeling of non-line-of-sight ultraviolet scattering channels for communication," *IEEE J. Sel. Areas Commun.* **27**, 1535–1544 (2009).
  22. C. Gabriel, M.-A. Khalighi, S. Bourennane, P. Léon, and V. Rigaud, "Monte-Carlo-based channel characterization for underwater optical communication systems," *J. Opt. Commun. Netw.* **5**, 1–12 (2013).
  23. W. Liu, D. Zou, P. Wang, Z. Xu, and L. Yang, "Wavelength dependent channel characterization for underwater optical wireless communications," in *Proceedings of IEEE International Conference on Signal Processing, Communications and Computing* (IEEE, 2014), pp. 895–899.
  24. T. A. Tsiftsis, H. G. Sandalidis, G. K. Karagiannidis, and M. Uysal, "Optical wireless links with spatial diversity over strong atmospheric turbulence channels," *IEEE Trans. Wireless Commun.* **8**, 951–957 (2009).
  25. F. Xu, M. A. Khalighi, and S. Bourennane, "Impact of different noise sources on the performance of PIN- and APD-based FSO receivers," in *Proceedings of the 11th International Conference on Telecommunications* (IEEE, 2011), pp. 211–218.
  26. P. Wang and Z. Xu, "Characteristics of ultraviolet scattering and turbulent channels," *Opt. Lett.* **38**, 2773–2775 (2013).